Water Air Soil Pollut (2010) 212:183–197
DOI 10.1007/s11270-010-0331-2

# An Application of Landsat-5TM Image Data for Water Quality Mapping in Lake Beysehir, Turkey

**Bilgehan Nas · Semih Ekercin · Hakan Karabörk · Ali Berktay · David J. Mulla**

Received: 8 September 2009 / Accepted: 13 January 2010 / Published online: 23 February 2010


**Abstract** The main goal of this study was to investigate spatial patterns in water quality in Lake Beysehir, which is the largest freshwater reservoir in Turkey, by using Landsat-5TM (Thematic Mapper) data and ground surveys. Suspended sediment (SS), turbidity, Secchi disk depth (SDD), and chlorophyll-a (chl-a) data were collected from 40 sampling stations in August, 2006. Spatial patterns in these parameters were estimated using bivariate and multiple regression (MR) techniques based on Landsat-5TM multispectral data and water quality sampling data. Single TM bands, band ratios, and combinations of TM bands were estimated and correlated with the measured water quality parameters. The best regression models showed that the measured and estimated values of water quality parameters were in good agreement ($0.60 < R^2 < 0.71$). TM3 provided a significant relationship ($R^2$=0.67, $p$<0.0001) with SS concentration. MR between chl-a and various combinations of TM bands showed that TM1, TM2, and TM4 are strongly correlated with measured chl-a concentrations ($R^2$=0.60, $p$<0.0001). MR of turbidity showed that TM1, TM2, and TM3 explain 60% ($p$< 0.0001) of the variance in turbidity. MR of SDD showed a strong relationship with measured SDD, with $R^2$=0.71 ($p$<0.0001) for the ratio TM1/TM3 and TM1 band combinations. The spatial distribution maps present apparent spatial variations of selected parameters for the study area covering the largest freshwater lake and drinking water reservoir in Turkey. Interpretation of thematic water quality maps indicated similar spatial distributions for SS, turbidity, and SDD. A large area in the middle portion of the lake showed very low chl-a concentrations as it is far from point and nonpoint sources of incoming nutrients. The trophic state index values were calculated from chl-a and SDD measurements. Lake Beysehir was classified as a mesotrophic or eutrophic lake according to chl-a or SDD parameters, respectively.

**Keywords** Satellite remote sensing · Water quality · In situ · Multiple regression · Landsat-5TM · Lake Beysehir

B. Nas (✉) · D. J. Mulla
Department of Soil, Water, and Climate,
University of Minnesota,
St. Paul, MN 55108, USA
e-mail: nasxx001@umn.edu

B. Nas · A. Berktay
Department of Environmental Engineering,
Selcuk University,
42075 Konya, Turkey

S. Ekercin
Department of Geodesy and Photogrammetry Engineering,
Aksaray University,
68100 Aksaray, Turkey

H. Karabörk
Department of Geodesy and Photogrammetry Engineering,
Selcuk University,
42075 Konya, Turkey

## 1 Introduction

Traditional lake water quality monitoring methods involving grab samples provide accurate data, but are usually expensive and time-consuming. This is particularly true for large water bodies like Beysehir Lake, which is the largest freshwater lake and drinking water reservoir in Central Anatolian Turkey.

Satellite technology can provide spatially unbiased information on certain characteristics of lakes across broad regions and has considerable potential to serve as a cost-effective complement to grab sample-based monitoring programs. Spectral brightness measured by satellite sensors is correlated with several water quality variables that affect a lake's optical properties. These include Secchi disk depth (SDD), turbidity, suspended solids, humic color, and chlorophyll-a concentration (Kloiber et al. 2002a, b). Optical and thermal sensors on boats, aircraft, and satellites provide both spatial and temporal information needed to understand changes in water quality parameters necessary for developing better management practices to improve water quality (Jensen 2000).

Several previous studies have shown strong relationships between brightness data collected by satellite systems and standard lake water quality variables (Nas et al. 2009; Lillesand et al. 1983; Nellis et al. 1998; Wang and Ma 2001; Östlund et al. 2001; Hedger et al. 2001; Koponen et al. 2002; Kloiber et al. 2002a, b; Hellweger et al. 2004; Brezonik et al. 2005; Duan et al. 2007; Ma and Dai 2005; Zhou et al. 2006; Tyler et al. 2006; Pulliainen et al 2001). The Landsat TM sensor has been used to a great extent to establish the relationships between water quality parameters of lakes and spectral reflectance as well as to assess and map the spatial distribution of some water quality parameters such as chlorophyll-a (chl-a), turbidity, SDD, and suspended sediment (SS; see Table 1).

The method most often used to demonstrate relationships between the spectral reflectance measured by sensors and water quality parameters collected in the field is regression analysis. The key in regression analysis is to select an appropriate regression method and independent variables that result in a high $R^2$ value. An $R^2$ value approaching 1 indicates good correlation between the predicted and measured data (Wang et al. 2006). Bivariate and multiple regression techniques have been used in many studies. Single TM bands, band ratios, and combinations of TM bands that represent spectral reflectance by water and substances in water have been entered in regression equations as independent variables. Even for the same water quality parameter, different independent variables have been employed. The best TM band or ratio often differs from one study to another (Brezonik et al. 2005).

Landsat 5, launched in 1984, continues to be operational. The Landsat-5TM sensor has seven spectral bands, the first four being of primary interest in this study. TM bands 5, 6, and 7 are not used to estimate the water characteristics of interest here.

This paper presents an application of water quality mapping through satellite and ground data. Lake Beysehir, Turkey was selected for study because it is the largest freshwater lake in Turkey and is increasingly impaired by point and nonpoint source pollutants. Landsat 5TM satellite image data source were collected for water quality mapping based on simultaneously obtained in situ lake water quality measurements such as SS, chl-a, turbidity, and SDD.

## 2 Methodology

### 2.1 Study Area and Water Sampling

Lake Beysehir is located 90 km from the city of Konya (between 31°17′ and 31°44′ E and 37°34′ and 37°59′ N) in Central Anatolia, Turkey (see Fig. 1). The area and the depth of the lake change with year and season. It has a surface area of about 654 km$^2$ and water volume of 4,159 million cubic meters when the height of above sea level is 1,123 m. Lake Beysehir (see Fig. 2) has a watershed area of about 4,140 km$^2$. This results in a watershed-to-lake ratio of about 6.3:1 (see Table 2).

The lake is of tectonic/karstic origin and is the most important drinking and irrigation water source for Central Anatolia. The lake's primary economic value is linked to fishery resources. Although it has some protected status, the lake has a number of problems such as declining water level due to inappropriate water policy, overgrowth of aquatic macrophytes in the lake ecosystem, uncontrolled fishing, urbanization, and water pollution.

Water samples were collected on August 22, 2006 at 40 points for this case study covering Lake

**Table 1** Satellite measurements of water quality in lakes

| Location | Surface area (km$^2$) | Mean depth (m) | Satellite/Sensor (s) | Parameter(s)/$R^2$ | Reference |
|---|---|---|---|---|---|
| Lakes in Minnesota, (USA) | 15 lakes | – | Landsat/TM | Chl-a: 0.88 | Brezonik et al. (2005) |
| | More than 10 500 lakes | – | Landsat 4-5-7/TM, MSS,ETM+ | SDD: 0.71-0.96 | Olmanson et al. (2008) |
| | ~500 lakes >0.1 km$^2$ | – | Landsat/TM, MSS | SDD: 0.71–0.92 | Kloiber et al. (2002a, b) |
| | ~500 lakes > 0.1 km$^2$ | – | Landsat/TM, MSS | SDD: 0.53–0.93 | Kloiber et al. (2002a, b) |
| Lake Beysehir, (Turkey) | 656 | 5.0 | ASTER/Terra | Chl-a: 0.863 | Nas et al. (2009) |
| Six Lakes, (Finland) | – | – | AISA | Chl-a: 0.945 | Pulliainen et al. (2001) |
| Lake Balaton, (Hungary) | 595 | 3.0 | Landsat/TM | Chl-a: 0.952 | Tyler et al. (2006) |
| Lake Chagan, (China) | 372 | 2.52 | Landsat/TM | Chl-a: 0.667 | Duan et al. (2007) |
| Lake Reelfoot, Tennessee and Kentucky, (USA) | 296.4 | 1.5 | Landsat-5/TM | SDD:0.588 Turbidity: 0.537 | Wang et al. (2006) |
| | | | | Chl-a: 0.705 | |
| | | | | SS: 0.522 | |
| Lake Taihu, (China) | 2,427.8 | 1.9 | Landsat ETM | Chl-a: 0.651 SS: 0.920 | Ma and Dai (2005) |
| Lake Taihu, (China) | 2,427.8 | 1.9 | Landsat-5/TM | SS: 0.63–0.74 | Zhou et al. (2006) |
| Lake Chagan, Lake Xinmiao, and Lake | 372 31 | 2.52 15 | Landsat / TM | Chl-a: 0.72 | Duan et al. (2008) |
| Kuli, (China) | 13 | 2 | | | |
| Lake Vänern and Vättern, (Swedish) | Vänern: 5,648 | 27 | Envisat/Meris | Chl-a: 0.52 | Alikas and Reinart (2008) |
| Lake Peipsi, Estonia and (Russia) | Vättern:1,856 Peipsi: 3,555 | 40 7 | | SS and CDOM: no correlation | |

Beysehir. At each sample site, a 2,500 ml water sample was collected with a vertical point water sampler at 50 cm below the surface. Polyethylene bottles had been cleaned by soaking in 10% nitric acid and rinsed with distilled water. At the sampling site, the bottles were rinsed twice with the water to be sampled prior to filling. Water samples were transported to the laboratory in a cooler box. All laboratory analyses were carried out within 24 h following sample collection. During the field work, a handheld global positioning system (GPS; Magellan SporTrak Color, accuracy <±3 m) was used to determine ground coordinates of water sampling points. Geographical locations of the sampled points are presented in Fig. 1.

SDD values were measured with a 20-cm diameter HydroBios disk with alternating black and white quadrants. The disk is lowered into a section of shaded water until it can no longer be seen and is then lifted back up until it can be seen once again. Averaging the two depths gives the clarity of the water. The extraction and measurement of the chlorophyll-a concentrations were made with acetone following the SM 10200 H-spectro-photometric method (APHA, AWWA, WEF 2005). Turbidity was measured using a Jenway turbidimeter by the SM 3230-B method (APHA, AWWA, WEF 2005). The SM 2540C method was used to measure the total suspended solids (APHA, AWWA, WEF 2005).

## 2.2 Data Used

The remotely sensed data used for water quality mapping were a Landsat-5TM multispectral image data acquired on August 30, 2006 (10:31 GMT; path/row, 178/34; Fig. 3). The Landsat TM instrument has

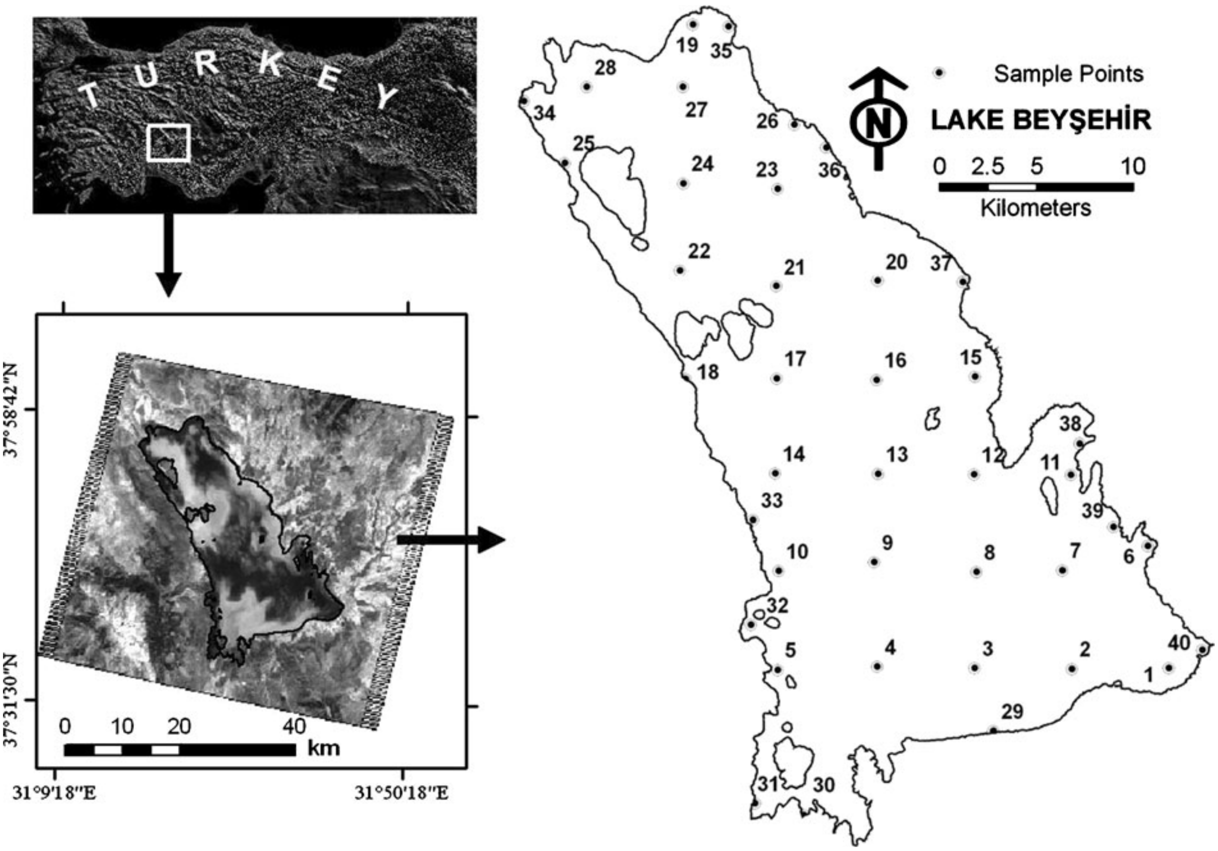


**Fig. 1** Location of the study area. *Numbers* on the lake surface refer to sampling locations

four spectral bands in the visible near-infrared VNIR (0.45–0.52, 0.52–0.60, and 0.63–0.69 µm and 0.76–0.90 µm to 30 m), two bands in the short wave infrared-SWIR (1.55–1.75 µm and 2.08–2.35 µm to 30 m), and one band in the thermal infrared TIR regions (10.4–12.5 µm to 120 m ground resolution). However, only VNIR and SWIR bands were used to develop multiple regression equations by correlating spectral radiance and water quality parameters. Image processing procedures were carried out using Erdas Imagine© and ASD ViewSpecPro© software packages. Additionally, topographic maps in the scale of 1:25,000 were used to get ground control points for the geometric correction process (Örmeci and Ekercin 2007).

### 2.3 Image Processing

In the image processing step, Landsat-5TM multispectral image data were first geometrically corrected by using 30 ground control points derived from 1:25,000 scale topographic maps. These data were resampled to 30-m pixel dimensions using a nearest neighbor algorithm and first-order polynomial transformation for sub-pixel accuracy (Dwivedi and Sreenivas 2002).

After geometric correction, the image was radiometrically corrected to convert digital numbers (DNs) to spectral radiance and to minimize atmospheric effects (Chavez 1996; Lillesand et al. 1983; Mather 1999). The equation proposed by Chander and Markham (2003) was used to convert DNs to spectral radiance.

$$L_\lambda = \mathrm{Gain}_\lambda \times \mathrm{DN}_\lambda + \mathrm{Bias}_\lambda \quad (1)$$

where $\mathrm{Gain}_\lambda$ [units of W/(m$^2$sr µm)/DN] and $\mathrm{Bias}_\lambda$ [units of W/(m$^2$sr µm)] are band-specific rescaling factors given in the header file of satellite data.

The next step is used to make the satellite data comparable with the spectral (in situ) measurements.

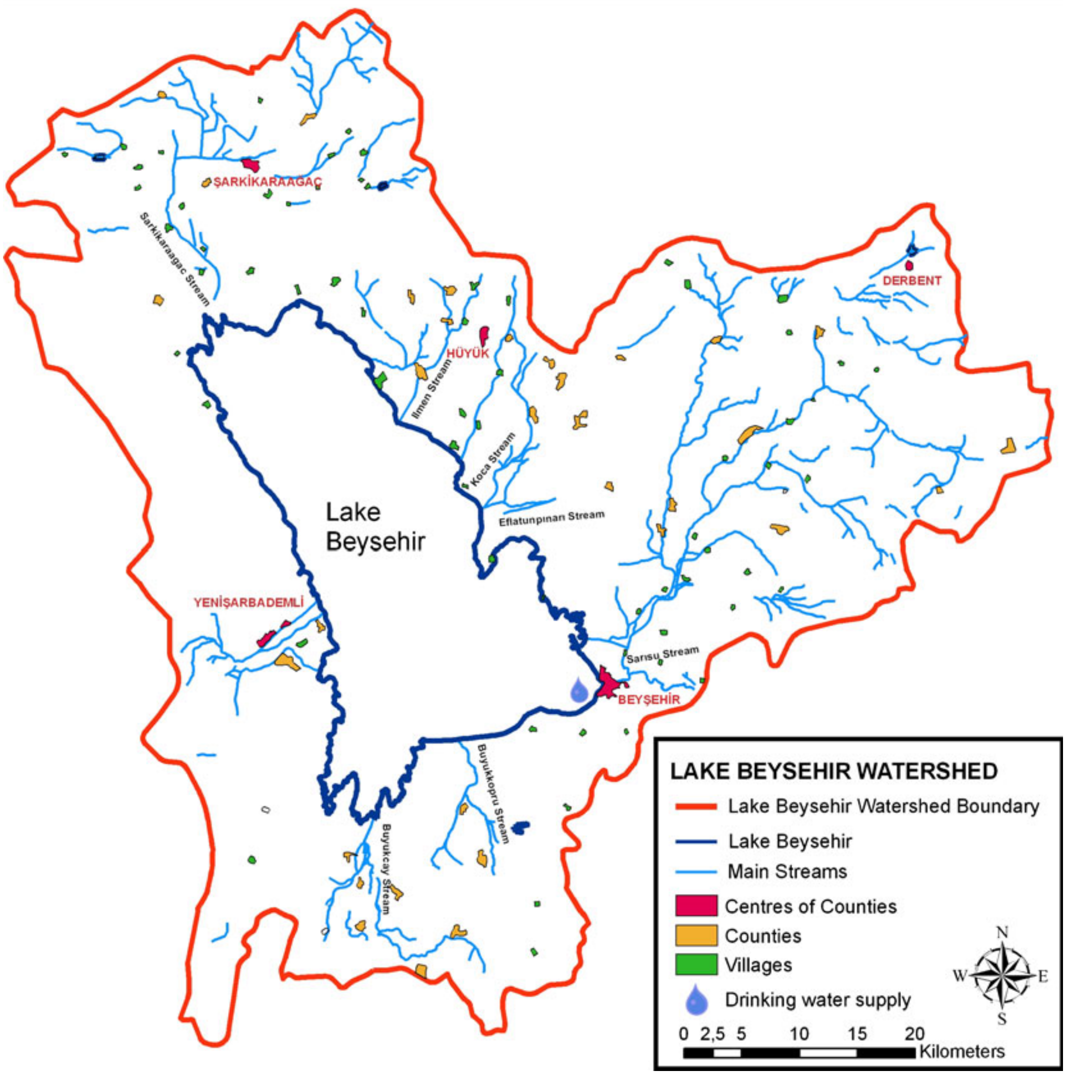


**Fig. 2** Lake Beysehir watershed

**Table 2** Lake Beysehir morphometric and watershed characteristics

| Parameter | Value |
|---|---|
| Mean depth (m) | 5 |
| Maximum depth (m) | 6.4 |
| Width range (km) | 10–24 |
| Length (km) | 45 |
| Watershed area ($km^2$) | 4,140 |
| Watershed-to-lake ratio | 6.3:1 |

We used, in this step, the following equation for conversion from radiance to at-satellite reflectance:

$$R = \frac{\pi \times L_\lambda \times d^2}{\mathrm{ESUN}_\lambda \times \mathrm{Cos}(\theta s)} \qquad (2)$$

where

- $R$ is the unitless planetary reflectance,
- $\pi$ is a constant (3.141592654),
- $L_\lambda$ id the spectral radiance at the sensor's aperture,
- $D$ is the earth–sun distance in astronomical units,
- $\mathrm{ESUN}_\lambda$ is the mean solar exoatmospheric irradiances (Chander and Markham (2003)

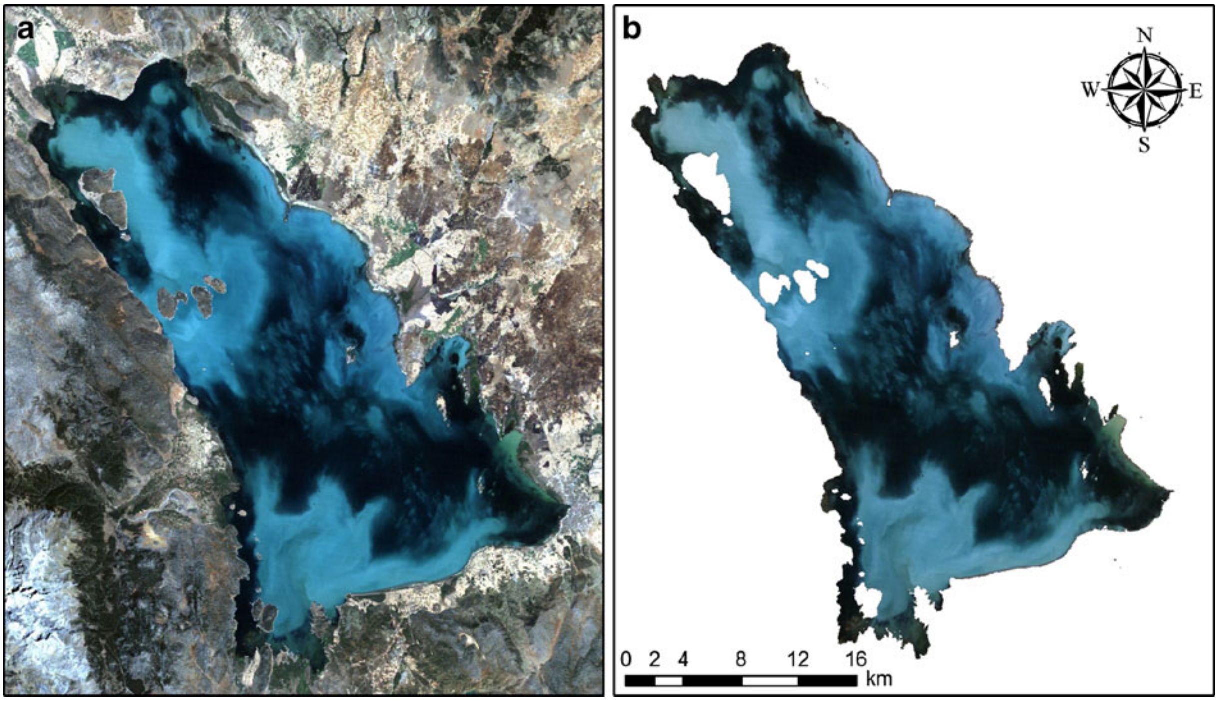


**Fig. 3** Lake Beysehir Landsat-5TM multispectral image data acquired on August 30, 2006

reported the values of $ESUN_\lambda$ and $d$ of the TM sensor), and

$\theta_s$ solar zenith angle in degrees (90° sun elevation).

## 2.4 Correlating Water Quality Parameters and Landsat-5TM Data

Kloiber et al. (2002a, b) found that ground observations within 1 day of the satellite image yielded the best calibrations. If ground observations and satellite imagery were collected at times differing by more than 1 day, some of the loss in correlation could be compensated by increasing the number of ground observations. Olmanson et al (2008) concluded that measurements taken within a few days (±3 to 10 days) of image acquisition provide strong relationships. This is because water clarity (Secchi depth) usually does not exhibit large and rapid fluctuations in a given lake during the relatively stable late summer index period. Chipman et al. (2004) had similar findings and determined that model parameter values did not change significantly with a wider time window.

In this study, a Landsat-5TM image was acquired on August 30, 2006 and water samples were collected in the Lake Beysehir on August 22, 2006. Between these 7 days, there was no rain or any other factor that caused fluctuations in lake water quality or depth.

In order to correlate reflectance and water quality parameters and to reduce errors in sample site locations, the average spectral reflectance of several pixels surrounding the sample pixel was used. Reddy (1997) reported a detailed study on the selection of optimum pixel configuration for the development of water quality models. Reddy (1997) found that the results of $t$ tests proved that 5×5 and 3×3 array sizes were optimum, and there was no significant difference between these two arrays (Wang et al. 2006). In order to remove (probable) errors resulting from GPS measurements during lake water quality sampling on Lake Beysehir, the average digital number of pixels in a 3 × 3 array surrounding the sample pixel was used for comparison between measured water quality parameters and Landsat-5TM multispectral imagery having a 30-m spatial resolution.

Based on a literature review of relationships between Landsat TM bands with spectral characteristics that have a high probability of predicting variations in SS, turbidity, chl-a, and SDD, we selected the following 28 bands or band combinations for statistical analysis:

TM1, TM2, TM3, TM4, (TM4/TM3), (TM2/TM1), (TM1/TM3), (TM3/TM1), (TM4/TM1), (TM3/TM2), (TM4/TM2), (TM4/TM3), (TM1 and TM2), (TM1 and TM3), (TM1 and TM4), (TM2 and TM3), (TM2 and TM4), (TM3 and TM4), (TM1, TM2, and TM3), (TM1, TM2, and TM4), (TM2, TM3, and TM4), (TM1, TM2, TM3, and TM4), [(TM1/TM4) + TM2], [(TM1/TM4) + TM1], [(TM1/TM3) + TM3], [(TM1/TM3) + TM2], [(TM1/TM3) + TM1], and [(TM4/TM1) + TM4].

In our study, only the first four TM bands were used for analysis because the long-wave bands provide little information for water quality assessment (Bilge et al. 2003; Dekker et al. 2002; Wang et al. 2006). Suspended sediment, turbidity, Secchi disk depth, and chlorophyll-a concentration were selected as water quality parameters because these parameters are optically active in terms of estimation from satellite remote sensing image data (Ekercin 2007). A significance level of $p$=0.05 was used to identify statistically significant relationships between measured water quality parameters and remote sensing bands or band combinations. Microsoft Excel and Analyse-it for Microsoft Excel were used for regression modeling and statistical analysis.

## 3 Results

For lake managers, the growing season mean and the worst-case conditions (maximum chl-*a* and minimum SDD) are of great interest for lake monitoring whether by ground-based measurement or satellite imagery. Selecting an image from the late summer allows for a direct estimate of the worst-case condition (Kloiber et al. 2002a, b). Therefore, the remotely sensed data used for this study were acquired on August 30, 2006. Table 3 shows water quality data from grab samples collected in Lake Beysehir on August 22, 2006.

The trophic state index is a vital factor to evaluate water quality conditions. Carlson's (1977) trophic state index (TSI) is based on the interrelationships between total phosphorus (TP), chlorophyll-a, and Secchi transparency. The latter two are amenable to measurement by satellite imagery. The TSI scale ranges from 0 to 100. The following breakpoints were used to define the trophic status of the lake: TSI≤40 "oligotrophic", ≥ 41 TSI<50 "mesotrophic", ≥ 50 TSI≤70 "eutrophic", and TSI≥70 "hypereutrophic." TSI values based on either chl-a or SDD can be calculated from the following equations (Carlson 1977):

**Table 3** Statistical properties of water quality data (August 22, 2006) of Lake Beysehir

| | Suspended Sediment (mg/l) | Turbidity (NTU) | Secchi disk depth (cm) | Chlorophyll-a (μg/l) |
|---|---|---|---|---|
| Mean | 4.51 | 7.89 | 189.19 | 4.25 |
| Min–Max | 0.1–15.5 | 0.59–18.90 | 35–530 | 0.56–15.51 |
| SD | 5.20 | 9.53 | 144.52 | 3.26 |

$$\text{Chlorophyll}-a\text{TSI} = 9.81 \times [\ln(\text{Chlorophyll} - a \text{ average}, \mu g/l)] + 30.6 \tag{3}$$

$$\text{Secchi disc depth TSI} = 60 - 14.41 \times \ln(\text{SDD average, meters}). \tag{4}$$

Mean TSI values for Lake Beysehir calculated using either chl-a or SDD measurements were 44.8 and 50.8, respectively. This means that on August 22, 2006, Lake Beysehir was mesotrophic according to chl-a concentration and eutrophic according to SDD.

Limnologists do not use turbidity and SS as trophic state indicators because they are not direct measures of algal abundance (Brezonik et al 2005). However, the Turkish Water Pollution and Control Regulation recommends that SS values not exceed 5 mg/l to control eutrophication on lakes (TWPCR 2008). SS concentrations in Lake Beysehir were in compliance with this recommendation, with a mean SS concentration of 4.51 mg/l.

### 3.1 Interpretation of the Bivariate and Multiple Regression Results

Regression equations relating Landsat data to water quality parameters (WQP) for Lake Beysehir are given in Tables 4 and 5. Table 4 gives results of

**Table 4** Determination coefficients ($R^2$) and bivariate regression equations for water quality parameters

| WQP | Regression equations | $R^2$ | Adjusted $R^2$ |
|---|---|---|---|
| Chl-a | $\mathrm{Chl-a} = -3.88 + 0.9315 \times TM4$ | 0.47 | 0.46 |
| | $\mathrm{Chl-a} = -1.438 + 41.66 \times (\mathrm{TM4/TM1})$ | 0.39 | 0.37 |
| Turbidity | $\mathrm{NTU} = -17.34 + 0.3788 \times \mathrm{TM1}$ | 0.36 | 0.34 |
| | $\mathrm{NTU} = -11.11 + 0.6535 \times \mathrm{TM2}$ | 0.46 | 0.45 |
| | $NTU = -11.83 + 0.9226 \times TM3$ | 0.57 | 0.56 |
| | $\mathrm{NTU} = -44.12 + 122.1 \times (\mathrm{TM2/TM1})$ | 0.52 | 0.51 |
| | $\mathrm{NTU} = -25.63 + 106.6 \times (\mathrm{TM3/TM1})$ | 0.48 | 0.46 |
| SDD | $\mathrm{SDD} = 379.5 - 3.595 \times \mathrm{TM1}$ | 0.45 | 0.43 |
| | $\mathrm{SDD} = 314.7 - 5.913 \times \mathrm{TM2}$ | 0.53 | 0.51 |
| | $\mathrm{SDD} = 316.6 - 8.128 \times \mathrm{TM3}$ | 0.57 | 0.56 |
| | $SDD = 617.3 - 1105 \times (TM2/TM1)$ | 0.58 | 0.57 |
| | $SDD = -262.6 + 125.1 \times (TM1/TM3)$ | 0.58 | 0.56 |
| SS | $\mathrm{SS} = -11 + 0.233 \times \mathrm{TM1}$ | 0.45 | 0.44 |
| | $\mathrm{SS} = -6.765 + 0.388 \times \mathrm{TM2}$ | 0.54 | 0.53 |
| | $SS = -7.102 + 0.543 \times TM3$ | 0.67 | 0.66 |
| | $\mathrm{SS} = -24.77 + 68.73 \times (\mathrm{TM2/TM1})$ | 0.56 | 0.55 |
| | $\mathrm{SS} = -14.46 + 60.31 \times (\mathrm{TM3/TM1})$ | 0.51 | 0.50 |

bivariate regression analyses, while Table 5 gives multivariate regression results.

### 3.1.1 Chlorophyll-a

Chlorophyll-a is an important parameter that affects lake trophic status. Spatial patterns of chl-a tend to be complex, being a result of biological as well as physical and chemical factors. Remote sensing is potentially useful at explaining the relative importance of biological and physical impacts on chl-a concentrations.

The broad TM bands cannot spectrally resolve the sharp spectral features arising from chl-a absorption. The chl-a absorption peak in the red region of the spectrum at 670 nm is only half contained in the red band of TM data; the peak near 700 nm is totally out of the TM red band. Therefore, different methods should be applied to the TM data to determine the chl-a level (Duan et al. 2007). Kloiber et al. (2002a, b) suggested that band combinations including ratios might provide useful relationships.

In our research, independent variables TM4 and TM4/TM1 have significant relationships with chlorophyll-a, explaining 47% and 39% of the variance in chlorophyll-a, respectively (Table 4). Multivariate regression of chl-a shows that the best regression model is $\mathrm{chl-a} = 7.394 - 0.377 \times \mathrm{TM1} + 0.536 \times \mathrm{TM2} + 0.732 \times \mathrm{TM4}$ (Table 5). Bands TM1, TM2, and TM4 explain 60% of the variance in chl-a (Fig. 4a).

### 3.1.2 Turbidity

Turbidity is a measure of the light-scattering properties of water. Turbidity of water is caused by the presence of suspended and dissolved matter such as clay, silt, finely divided organic matter, plankton, other microscopic organisms, organic acids, and dyes.

Independent variables TM3, TM2/TM1, and TM3/TM1 are three variables that have significant relationships with turbidity, with 57%, 52%, and 48% of the variance in turbidity being explained, respectively. TM3 is the best variable based on the highest percent of variance explained in turbidity.

Multivariate regression of turbidity shows that $\mathrm{Turbidity} = -0.221 - 0.463 \times \mathrm{TM1} + 0.722 \times \mathrm{TM2} + 0.841 \times \mathrm{TM3}$ is the best regression equation (see Table 5). Bands TM1, TM2, and TM3 explain 60% of the variance in turbidity (see Fig. 4b). When turbidity is the dependent variable and the three bands of TM are the independent variables, the relationship between TM2, TM3, and turbidity is positive, while the relationship between TM1 and turbidity is negative.

**Table 5** Determination coefficients ($R^2$) and multiple regression equations for water quality parameters

| WQP | Regression equations | $R^2$ | Adjusted $R^2$ |
|---|---|---|---|
| Chl-a | $\mathrm{Chl-a} = -1.663 - 0.037 \times \mathrm{TM1} + 0.958 \times \mathrm{TM4}$ | 0.50 | 0.47 |
| | $\mathrm{Chl-a} = -3.645 - 0.023 \times \mathrm{TM3} + 0.961 \times \mathrm{TM4}$ | 0.48 | 0.45 |
| | $\mathrm{Chl-a} = -2.195 - 0.170 \times \mathrm{TM2} + 0.192 \times \mathrm{TM3} + 0.835 \times \mathrm{TM4}$ | 0.50 | 0.46 |
| | $Chl - a = 7.394 - 0.377 \times TM1 + 0.536 \times TM2 + 0.732 \times TM4$ | 0.60 | 0.56 |
| | $Chl - a = 7.428 - 0.379 \times TM1 + 0.544 \times TM2 - 0.006 \times TM3 + 0.735 \times TM4$ | 0.60 | 0.55 |
| | $\mathrm{Chl-a} = -3.857 + 14.81 \times (\mathrm{TM4/TM1}) + 0.697 \times \mathrm{TM4}$ | 0.49 | 0.46 |
| Turbidity | $\mathrm{NTU} = 9.823 - 0.891 \times \mathrm{TM1} + 1.976 \times \mathrm{TM2}$ | 0.55 | 0.53 |
| | $\mathrm{NTU} = -7.495 - 0.139 \times \mathrm{TM1} + 1.152 \times \mathrm{TM3}$ | 0.59 | 0.56 |
| | $\mathrm{NTU} = -11.1 - 0.183 \times \mathrm{TM2} + 1.138 \times \mathrm{TM3}$ | 0.58 | 0.56 |
| | $\mathrm{NTU} = -12.85 + 0.902 \times \mathrm{TM3} + 16.65 \times \mathrm{TM4}$ | 0.58 | 0.55 |
| | $NTU = -0.221 - 0.463 \times TM1 + 0.722 \times TM2 + 0.841 \times TM3$ | 0.60 | 0.56 |
| | $NTU = 0.693 - 0.476 \times TM1 + 0.723 \times TM2 + 0.872 \times TM3 - 0.086 \times TM4$ | 0.60 | 0.55 |
| | $\mathrm{NTU} = -14.17 + 0.515 \times (\mathrm{TM1/TM3}) + 0.953 \times \mathrm{TM3}$ | 0.57 | 0.55 |
| SDD | $\mathrm{SDD} = 387 - 5.492 \times \mathrm{TM2} - 9.673 \times \mathrm{TM4}$ | 0.61 | 0.58 |
| | $\mathrm{SDD} = 352.7 - 7.496 \times \mathrm{TM3} - 5.709 \times \mathrm{TM4}$ | 0.60 | 0.57 |
| | $\mathrm{SDD} = 376.1 - 3.343 \times \mathrm{TM2} - 3.13 \times \mathrm{TM3} - 7.914 \times \mathrm{TM4}$ | 0.62 | 0.57 |
| | $\mathrm{SDD} = 386.1 - 0.396 \times \mathrm{TM1} - 2.562 \times \mathrm{TM2} - 3.392 \times \mathrm{TM3} - 8.031 \times \mathrm{TM4}$ | 0.62 | 0.56 |
| | $\mathrm{SDD} = 11 - 4.421 \times (\mathrm{TM1/TM3}) + 70.03 \times \mathrm{TM3}$ | 0.64 | 0.61 |
| | $\mathrm{SDD} = -26.55 + 83.47 \times (\mathrm{TM1/TM3}) - 3.429 \times \mathrm{TM2}$ | 0.69 | 0.67 |
| | $SDD = -16.89 + 93.84 \times (TM1/TM3) - 2.162 \times TM1$ | 0.71 | 0.68 |
| SS | $\mathrm{SS} = 1.594 - 0.356 \times \mathrm{TM1} + 0.916 \times \mathrm{TM2}$ | 0.59 | 0.57 |
| | $SS = -5.738 - 0.044 \times TM1 + 0.616 \times TM3$ | 0.67 | 0.66 |
| | $SS = -6.762 - 0.086 \times TM2 + 0.644 \times TM3$ | 0.67 | 0.66 |
| | $SS = -5.776 - 0.042 \times TM1 - 0.004 \times TM2 + 0.617 \times TM3$ | 0.67 | 0.65 |
| | $SS = -5.275 - 0.049 \times TM1 - 0.003 \times TM2 + 0.634 \times TM3 - 0.047 \times TM4$ | 0.67 | 0.64 |

### *3.1.3 Secchi Disk Depth*

SDD is the most commonly measured trophic state indicator and is strongly correlated with the responses in the blue and red bands of Landsat TM/ETM + data (Kloiber et al. 2002a, b).

There were six locations in Lake Beysehir where the measured SDD values exceeded 4 m. These data were removed for the regression analyses. We determined that when SDD is more than 4 m, the relationship between SDD and Landsat TM data decreases significantly.

Independent variables TM2/TM1 and TM1/TM3 have the closest relationship with SDD in Lake Beysehir (see Table 4) and account for 58% of the variance in SDD. TM3 is the second best predictor and accounts for 57% of the variance.

Multivariate regression of SDD as the dependent variable shows that $\mathrm{SDD} = -16.89 + 93.84 \times (\mathrm{TM1/TM3}) - 2.162 \times \mathrm{TM1}$ explains the greatest amount of variance in SDD (Table 5). Both TM1/TM3 and TM1 explain 71% of the variance in SDD (see Fig. 4c). The relationship between TM1/TM3 and SDD is positive, while the relationship between TM1 and SDD is negative. TM1/TM3 and TM2 are the second best predictors and account for 69% of the variance. If we use locations where SDD data exceed 4 m, $R^2$ values decrease from 0.57 to 0.42 for the TM3 band. Multivariate regression of SDD decreases from 0.71 to 0.56 for the TM1/TM3 and TM1 band combination.

### *3.1.4 Suspended Sediment*

Remotely sensed reflectance measured in the red portion (600–700 nm, like Landsat TM3) of the visible spectrum is suitable for estimating concentrations of suspended matter in inland waters (Zhou et al. 2006). TM3 values had the strongest relationship

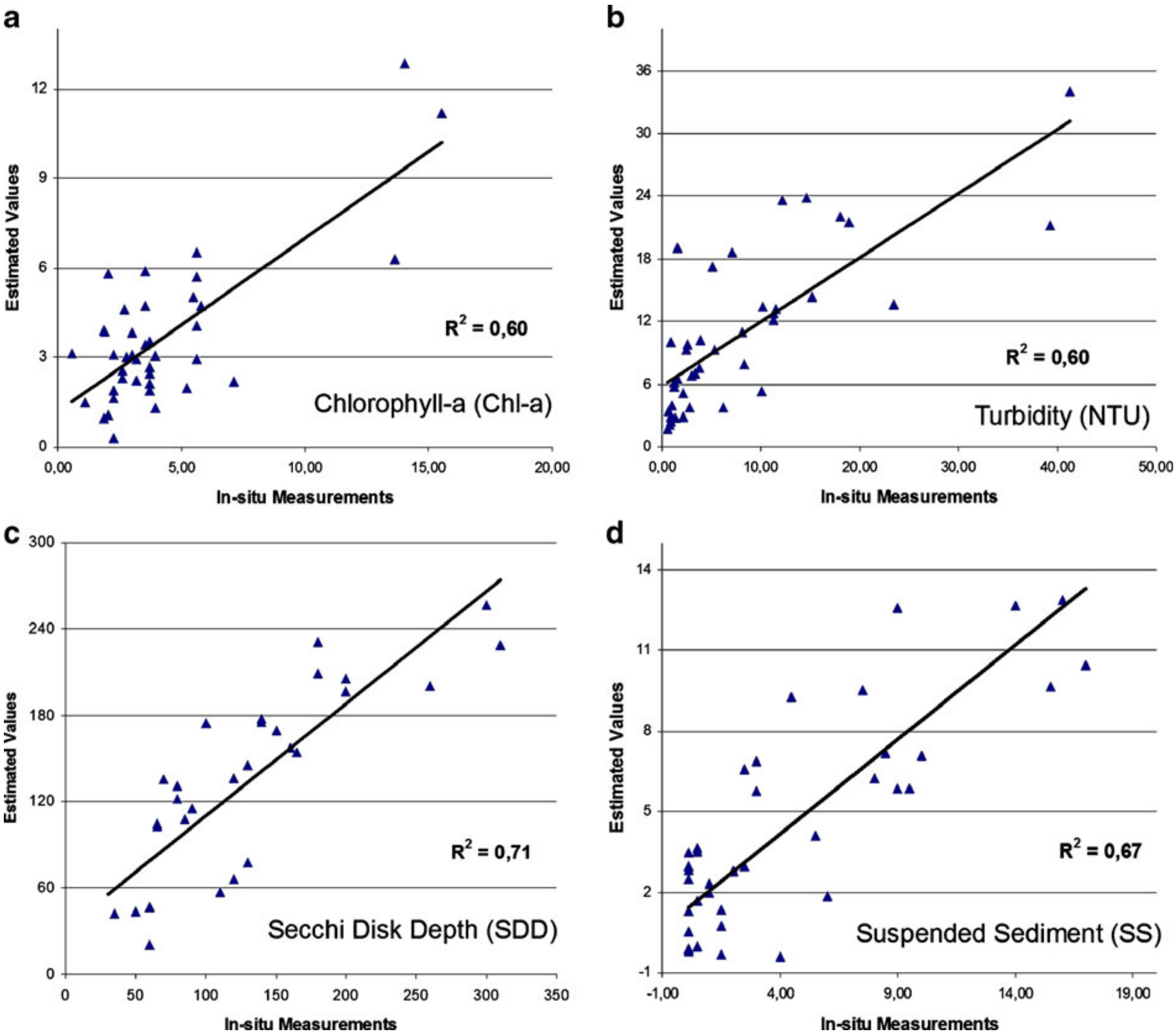


**Fig. 4** Comparison of satellite-estimated and in situ measurement water quality parameters for Landsat-5TM image from August 2006

with measured SS concentrations among all Landsat bands tested (see Table 3). This result is consistent with several previous investigations (Dekker et al. 2002; Bilge et al. 2003; Tyler et al. 2006).

In our research, there is a significant relationship between TM3 and SS (see Table 4). TM3 alone is significantly correlated with SS and explains 67% of the variance in SS. Other variables such as TM2 and TM1 also contribute significantly to the variance in SS with $R^2$ values of 54% and 45%, respectively. A near-infrared band, like TM4, would be well suited for determining the SS concentrations in suspended sediment-dominated lake water with relatively low phytoplankton algae concentrations. In this study, the importance of TM4 to SS is only 11%. Independent variables TM2/TM1 and TM3/TM1 are two variables that have significant relationships with SS, with 56% and 51% of the variance in SS being explained, respectively (see Table 4). Independent variables TM1, TM2, TM3, and TM4 together explain 67% of the variance in SS. As mentioned earlier, this is the same percentage that is explained by TM3 alone. Thus, TM3 alone is sufficient for explaining the variability in SS concentrations in Lake Beysehir (see Tables 4 and 5 and Fig. 4d).

The best fitting regression equations for Lake Beysehir water quality parameters were (Tables 3 and 4):

$$\mathrm{chl-a} = 7.394 - 0.377 \times \mathrm{TM1} + 0.536 \times \mathrm{TM2} + 0.732 \times \mathrm{TM4} \quad (5)$$

$$\mathrm{Turbidity} = -0.221 - 0.463 \times \mathrm{TM1} + 0.722 \times \mathrm{TM2} + 0.841 \times \mathrm{TM3} \quad (6)$$

$$\mathrm{SDD} = -16.89 + 93.84 \times (\mathrm{TM1}/\mathrm{TM3}) - 2.162 \times \mathrm{TM1} \quad (7)$$

$$\mathrm{SS} = -7.102 + 0.543 \times \mathrm{TM3}. \quad (8)$$

Figure 4 shows the comparison of satellite-estimated and in situ measurement water quality parameters from Eqs. 5, 6, 7, and 8.

### 3.2 Evaluation of Spatial Pattern of Water Quality

Best regression equations were used to estimate the value of each water quality parameter at all locations where digital numbers were calculated in Lake Beysehir. The resulting water quality parameters were then classified into groups and used to depict spatial patterns in chl-a, turbidity, Secchi disk depth, and SS across Lake Beysehir (see Fig. 5).

Spatial patterns in chl-a predicted from remote sensing are shown in Fig. 5a. As can be seen Figs. 2 and 5a, areas showing the highest concentration of chl-a correspond to areas which receive untreated domestic wastewater via streams from villages in adjoining areas of the lake. Of particular importance is Sarkikaraagac stream which discharges pollution from many point sources at the northern end of the lake. The highest chl-a concentrations (see Figs. 1 and 5a) occurred near stations 25, 28, and 34 in the northern portion of the lake. Prolific growths of macrophytes were observed near the northern, southern, and eastern banks of the lake due to wastewater discharges and agricultural runoff. A large area in the middle portion of the lake shows very low chl-a concentrations as it is far from point and nonpoint sources of incoming nutrients. The areas closer to shorelines where there is human activity have relatively poor water quality as compared to the areas far away from the shorelines.

Spatial distributions for turbidity and SDD (see Fig. 5b, c) are similar to spatial distributions in SS concentration across Lake Beysehir. These three water quality parameters (SS, turbidity, and SDD) are related to clarity of lakes, and it is not surprising that they have similar spatial distributions. Clarity of water decreases in the presence of suspended and dissolved matter such as clay, silt, organic matter, and plankton. In this case, SS and turbidity concentrations of water increase, while SDD decreases.

The distribution of SS concentrations across Lake Beysehir is shown in Fig. 5d. SS concentrations are relatively low in the middle of the lake. Around stations 28, 24, and 22 which are located north and east of Mada island and around the islands (Igdeli, Aygır, and Orta), high concentrations of SS were found. Around stations 2, 3, and 29 in the southern and 15, 26, 36, and 37 in the eastern portions of the lake, high SS concentrations were observed. These stations were located near shoreland (see Figs. 1 and 5). The spatial patterns in SS, turbidity, and SDD are related to the location of streams that discharge into Lake Beysehir. These streams include Sarkikaraagac stream in the north, Kocacay and Eflatun streams in the east, and Soguksu, Buyukkopru, and Sogutlubogaz streams in the south of the lake (see Fig. 2). Stream discharge contains large quantities of sediment as well as untreated domestic wastewater.

## 4 Discussion and Conclusions

One of the prime management issues for inland lakes is trophic status, and of the three most common indicators of trophic state—TP, chl-*a*, and SDD—the latter two are amenable to measurement by satellite imagery.

Based on literature-based relationships between measured SS, turbidity, chl-a, and SDD and bands of Landsat TM, we studied 29 various combinations of bands to correlate with water quality parameters. The best TM band or ratio often differs from one study to another (Brezonik et al. 2005). Therefore, single TM bands, band ratios, and combinations of TM bands were statistically evaluated for their ability to predict water quality parameters.

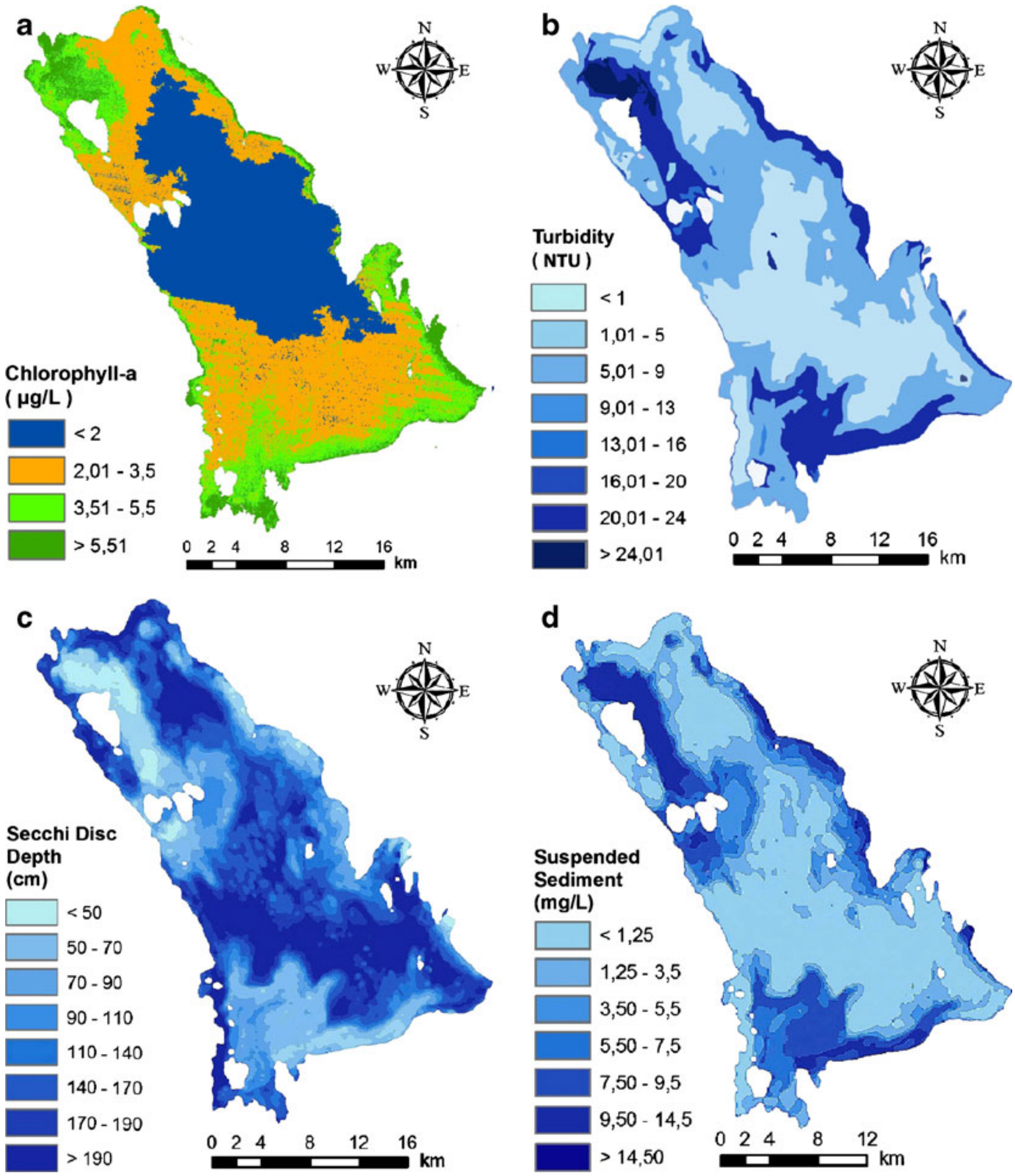


**Fig. 5** Distribution of chl-a, turbidity, Secchi disk depth, and suspended sediment parameters over the study area on 30 August 2006

SS, turbidity, chl-a, and SDD are strongly correlated with Landsat TM image reflectance data. Regression equations relating Landsat TM data and water quality parameters produced generally strong relationships, with $R^2$ values ranging from 0.60 to 0.71.

Jensen (2000) and Dekker et al. (2002) have found that TM4 has a good relationship with SS and would be suitable for estimating SS. TM2, TM3, and TM4 values have previously been used by Wang et al. (2006) to predict SS concentrations in lakes. Overall, the three variables explain 52.2% of the variance in SS. Zhou et al. (2006) reported that TM4 and TM4/TM1 are significantly correlated with SS for lakes with relatively low concentrations of phytoplankton algae. Zhou et al. (2006) also indicated that TM3 is good ($R^2$=0.63) for estimating the SS in summer and autumn, and it is feasible to apply the linear regression model using TM3 to estimate SS concentrations across time in Lake Taihu even if no in situ data were available. Tyler et al. (2006) mapped the distribution of SS with Landsat TM band 3 in Lake Balaton.

Our results confirm the findings of Bilge et al. (2003), Tassan (1997), Dekker et al. (2002), Tyler et al. (2006), and Zhou et al. (2006) in which TM3 had the strongest relationship with SS concentrations. TM3 is a significant ($R^2$=0.67) predictor of SS concentrations for Lake Beysehir.

Brezonik et al. (2005) reported that the ratio of TM1 to TM3 produced the strongest relationship ($R^2$=0.88) with chl-a concentrations on 15 Minnesota lakes. Wang et al. (2006) found that the ratio of TM3 to TM2 had a significant relationship with chl-a ($R^2$= 0.53). Multiple regressions between chl-a and various combinations of TM bands showed that TM2 and TM3 are significant ($R^2$=0.70). Duan et al. (2007) found the best regression model had an $R^2$ value of 0.67 when the band ratio TM4/TM3 was used to predict chl-a concentrations in Lake Chagan. Nas et al. (2009) reported high agreement ($R^2$=0.86) using multiple regression technique and Terra ASTER satellite data in Lake Beysehir.

In this research, TM4 and multivariate regression of TM1, TM2, and TM4 had significant relationships with chl-a and explained 47% and 60% of the variance in chl-a, respectively.

Wang et al. (2006) found that the ratio of TM3 to TM2 has a significant relationship with turbidity ($R^2$=0.37). Multiple regression models between turbidity and various combinations of TM bands showed (Table 3) that TM2 and TM3 are significant ($R^2$=0.54).

In our research, TM3 is a significant ($R^2$=0.57) predictor of turbidity as well as SS. The best relationship for turbidity was the combination of bands TM1, TM2, and TM3 ($R^2$=0.60).

Kloiber et al. (2002a, b) produced generally strong relationship, with $R^2$ values ranging from 0.53 to 0.93, using log-transformed SDD data as the dependent variable and TM1 and the TM1/TM3 ratio as independent variables in nearly 500 lakes in Minnesota. Thirteen Landsat MSS and TM images over the period 1973–1998 were used for the analysis. Olmanson et al. (2008) obtained strong relationships (average $R^2$ values of 0.83 ranging from 0.71 to 0.96) using log-transformed SDD data and the TM1 and TM1/TM3 ratio on more than 10,500 lakes at 5-year intervals over the period 1985–2005 in Minnesota. More than 100 Landsat MSS, TM, ETM + images from 37 dates were used in the research. Wang et al. (2006) reported that the ratio of TM3 to TM2 has significant relationships with SDD ($R^2$=0.43). Multiple regressions between SDD and various combinations of TM bands shows that in this study, TM2 and TM3 are significantly correlated with SDD (Table 3; $R^2$=0.59). In this study, the maximum measured SDD value is 33 cm.

Our results confirm the findings of Kloiber et al. (2002a, b), Brezonik et al. (2005), and Olmanson et al. (2008) in which combinations of band TM1 with the band ratio TM1/TM3 had a significant relationship with SDD in Lake Beysehir. $\mathrm{SDD} = -16.89 + 93.84 \times (\mathrm{TM1}/\mathrm{TM3}) - 2.162 \times \mathrm{TM1}$ was the regression equation that explained the greatest amount of variance ($R^2$=0.71) in SDD.

Spatial patterns were estimated using regression analysis combined with remote sensing data for selected water quality parameters in Lake Beysehir, Turkey. The results show that areas close to shorelines where there is point and nonpoint source pollution arising from human activity have relatively poor water quality as compared to the areas far away from the shorelines.

Lake Beysehir was mesotrophic according to chl-a concentration and eutrophic according to SDD on August 22, 2006. Turbidity and SS were not used as trophic state indicators. TWPCR recommends that SS values not exceed 5 mg/l to control eutrophication on lakes. SS concentrations in Lake Beysehir were in compliance with this recommendation. For turbidity, the value of 5 NTU is recommended with the maximum contaminant level (MCL) of 25 NTU by Turkish Standard Institute (TSE 1997). The minimum and maximum values of turbidity were measured as 0.59 and 18.90 NTU, respectively. Average turbidity concentration is 7.89 NTU and exceeds the recommended of 5 NTU indicated by the TSE. There was no well in which the turbidity exceeds the MCL of 25 NTU given in the Turkish Standards.

**Acknowledgement** This research was funded by The Scientific and Technological Research Council of Turkey-TUBITAK (grant no. 105Y086) and Selcuk University Scientific Research Fund-SUAF (grant no. 2004/102).

## References


Alikas, K., & Reinart, A. (2008). Validation of the MERIS products on large European lakes: Peipsi, Vänern and Vättern. *Hydrobiologia, 599*, 161–168.

APHA, AWWA, & WEF. (2005). *Standard methods for the examination of water and wastewater* (21st ed.). Washington: American Public Health Association/American Water Works Association/Water Environment Federation.

Bilge, F., Yazici, B., Dogeroglu, T., & Ayday, C. (2003). Statistical evaluation of remotely sensed data for water quality monitoring. *International Journal of Remote Sensing, 24*, 5317–5326.

Brezonik, P., Menken, K. D., & Bauer, M. (2005). Landsat-based remote sensing of lake water quality characteristics, including chlorophyll and colored dissolved organic matter (CDOM). *Lake and Reservoir Management, 21*(4), 373–382.

Carlson, R. E. (1977). A trophic state index for Lakes. *Limnology and Oceanography, 22*(2), 361–369.

Chipman, J. W., Lillesand, T. M., Schmaltz, J. E., Leale, J. E., & Nordheim, M. J. (2004). Mapping lake water clarity with Landsat images in Wisconsin, USA. *Canada Journal of Remote Sensing, 30*, 1–7.

Chander, G., & Markham, B. (2003). Revised Landsat-5 TM radiometric calibration procedures and postcalibration dynamic ranges. *IEEE Transactions on Geoscience and Remote Sensing, 41*, 2674–2677.

Chavez, P. S. (1996). Image-based atmospheric corrections—Revisited and improved. *Photogrammetric Engineering and Remote Sensing, 62*, 1025–1036.

Dekker, A. G., Vos, R. J., & Peters, S. W. M. (2002). Analytical algorithms for lake water TSM estimation for retrospective analysis of TM and SPOT sensor data. *International Journal of Remote Sensing, 23*, 15–35.

Duan, H., Zhang, Y., Zhang, B., Song, K., & Wang, Z. (2007). Assessment of chlorophyll-a concentration and trophic state for Lake Chagan using Landsat TM and field spectral data. *Environmental Monitoring and Assessment, 129*, 295–308.

Duan, H., Zhang, Y., Zhang, B., Song, K., Wang, Z., & Liu, D. (2008). Estimation of chlorophyll-a concentration and trophic states for inland lakes in Northeast China from Landsat TM data and field spectral measurements. *International Journal of Remote Sensing, 29*(3), 767–786.

Dwivedi, R. S., & Sreenivas, K. (2002). The vegetation and waterlogging dynamics as derived from spaceborne multispectral and multitemporal data. *International Journal of Remote Sensing, 23*, 2729–2740.

Ekercin, S. (2007). Water quality retrievals from high resolution IKONOS multispectral imagery: A case study in Istanbul, Turkey. *Water, Air & Soil Pollution, 183*, 239–251.

Hedger, R. D., Atkinson, P. M., & Malthus, T. J. (2001). Optimizing sampling strategies for estimating mean water quality in lakes using geostatistical techniques with remote sensing. *Lakes & Reservoirs: Research and Management, 6*, 279–288.

Hellweger, F. L., Schlosser, P., Lall, U., & Weissel, J. K. (2004). Use of satellite imagery for water quality studies in New York Harbor. *Estuarine, Coastal and Shelf Science, 61*, 437–448.

Koponen, S., Pulliainen, J., Kallio, K., & Hallikainen, M. (2002). Lake water quality classification with airborne hyperspectral spectrometer and simulated MERIS data. *Remote Sensing of Environment, 79*, 51–59.

Jensen, J. R. (2000). *Remote sensing of the environment: An earth resource perspective*. Upper Saddle River: Prentice Hall.

Kloiber, S. M., Brezonik, P. L., & Bauer, M. E. (2002). Application of Landsat imagery to regional-scale assessments of lake clarity. *Water Research, 36*, 4330–4340.

Kloiber, S. M., Brezonik, P. L., Olmanson, L. G., & Bauer, M. E. (2002). A procedure for regional lake water clarity assessment using Landsat multispectral data. *Remote Sensing of Environment, 82*, 38–47.

Lillesand, T. M., Johnson, W. L., Deuell, R. L., Lindstrom, O. M., & Meisner, D. E. (1983). Use of Landsat data to predict the trophic state of Minnesota lakes. *Photogrammetric Engineering and Remote Sensing, 49*, 219–229.

Ma, R., & Dai, J. (2005). Investigation of chlorophyll-a and total suspended matter concentrations using Landsat ETM and field spectral measurement in Taihu Lake, China. *International Journal of Remote Sensing, 26*(13), 2779–2787.

Mather, P. (1999). Computer Processing of Remotely Sensed Images, John Wiley & Sons, Chichester, UK.

Nas, B., Karabork, H., Ekercin, S., & Berktay, A. (2009). Mapping chlorophyll-a through in-situ measurements and Terra ASTER satellite data. *Environmental Monitoring and Assessment, 157*, 375–382.

Nellis, M. D., Harrington, J. A., & Wu, J. (1998). Remote sensing of temporal and spatial variations in pool size, suspended sediment, turbidity, and Secchi depth in Tuttle Creek Reservoir, Kansas: 1993. *Geomorphology, 21*, 281–293.

Olmanson, L. G., Bauer, M. E., & Brezonik, P. L. (2008). A 20-year Landsat water clarity census of Minnesota's 10, 000 Lakes. *Remote Sensing of Environment, 122*(11), 4086–4097.

Örmeci, C., & Ekercin, S. (2007). An assessment of water reserve change in the Salt Lake, Turkey through multi-temporal Landsat imagery and real-time ground surveys. *Hydrological Processes, 21*, 1424–1435.

Östlund, C., Flink, P., Strombeck, N., Pierson, D., & Lindell, T. (2001). Mapping of the water quality of Lake Erken, Sweden, from imaging spectrometry and Landsat thematic mapper. *Science of the Total Environment, 268*, 139–154.

Pulliainen, J., Kallio, K., Eloheimo, K., Koponen, S., Servomaa, H., Hannonen, T., et al. (2001). A semi-operative approach to lake water quality retrieval from remote sensing data. *Science of the Total Environment, 28*, 79–93.

Reddy, M. A. (1997). A detailed statistical study on selection of optimum IRS LISS pixel configuration for development of water quality models. *International Journal of Remote Sensing, 18*, 2559–2570.

Tassan, S. (1997). A numerical model for the detection of sediment concentration in stratified river plumes using Thematic Mapper data, *International Journal of Remote Sensing, 18*(12), 2699-2705.

TWPCR. (2008). Water pollution control regulation. Ministry of Environment and Forestry of Turkey, Official Gazette No. 26786, Ankara, Turkey

TSE. (1997). Drinking Water Turkish Standards. Turkish Standards (TSE-266), Ankara, Turkey

Tyler, A. N., Svab, E., Preston, T., Présing, M., & Kovács, W. A. (2006). Remote sensing of the water quality of shallow lakes: A mixture modelling approach to quantifying phytoplankton in water characterized by high-suspended sediment. *International Journal of Remote Sensing, 27*(8), 1521–1537.

Wang, F., Luoheng, H., Hsiang-Te, K., & Roy, B. V. A. (2006). Applications of Landsat-5 TM imagery in assessing and mapping water quality in Reelfoot Lake, Tennessee. *International Journal of Remote Sensing, 27*(23), 5269–5283.

Wang, X. J., & Ma, T. (2001). Application of remote sensing techniques in monitoring and assessing the water quality of Taihu Lake. *Bulletin of Environmental Contamination and Toxicology, 67*, 863–870.

Zhou, W., Wang, S., Zhou, Y., & Troy, A. (2006). Mapping the concentrations of total suspended matter in Lake Taihu, China, using Landsat-5 TM data. *International Journal of Remote Sensing, 27*(6), 1177–1191.